ARTICLE

Check for updates

Flexible organic thin-film transistor immunosensor printed on a one-micron-thick film

Tsukuru Minamiki [1,3], Tsuyoshi Minami[1,2✉], Yi-Pu Chen[1], Taisei Mano[1], Yasunori Takeda [1], Kenjiro Fukuda [1,4] & Shizuo Tokito[1✉]

Flexible and printed biosensor devices can be used in wearable and disposable sensing systems for the daily management of health conditions. Organic thin-film transistors (OTFTs) are promising candidates for constructing such systems. Moreover, the integration of organic electronic materials and biosensors is of extreme interest owing to their mechanical and chemical features. To this end, the molecular recognition chemistry-based design for the interface between sensor devices and analyte solution is crucial to obtain accurate and reproducible sensing signals of targets, though little consideration has been given to this standpoint in the field of device engineering. Here, we report a printed OTFT on a 1 µm-thick film functionalized with a sensing material. Importantly, the fabricated device quantitatively responds to the addition of a protein immunological marker. These results provide guidelines for the development of effective healthcare tools.

[1] Research Center for Organic Electronics (ROEL), Graduate School of Science and Engineering, Yamagata University, 4-3-16 Jonan, Yonezawa, Yamagata 992-8510, Japan. [2] Institute of Industrial Science, The University of Tokyo, 4-6-1 Komaba, Meguro-ku, Tokyo 153-8505, Japan. [3] Present address: Health and Medical Research Institute, National Institute of Advanced Industrial Science and Technology (AIST), 1-1-1 Higashi, Tsukuba, Ibaraki 305-8566, Japan. [4] Present address: Thin-Film Device Laboratory, RIKEN, 2-1 Hirosawa, Wako 351-0198 Saitama, Japan. ✉email: tminami@iis.u-tokyo.ac.jp; tokito@yz.yamagata-u.ac.jp

Related to the global increase in the incidence of lifestyle diseases, a rise in health awareness, and public hygiene resulting from globalization, the development of point-of-care testing (POCT) technologies has attracted attention for the management of health conditions based on quantitative and chronological data[1,2]. In particular, the medical industry is devoting a lot of effort toward the realization of rapid and disposable assays to detect immunological markers or viruses for preventing the spread of serious infectious diseases or inflammations. For these purposes, wearable biosensors are of great interest because they can inspect our bioactivity unobtrusively and continuously[3,4]. To achieve the real-time monitoring of health conditions utilizing wearable sensors, the devices should fulfill the following requirements: (1) To evaluate bioactivity in accordance with quantitative data, devices should linearly respond to changes in biomarker levels. (2) For the qualitative investigation of health conditions, detection units in wearable devices must be functionalized with specific recognition materials for biomarkers. (3) To maintain cleanness on human skin or tissues, wearable devices should be disposable. This point is also significant in protecting against the spread of secondary infections from patients to medical workers. Hence, low-cost processes should be focused on in the development of biosensing devices so that biosensors can be realized as a sufficiently low cost for their regular replacement.

To satisfy the above-mentioned requirements for the development of wearable biosensors, organic thin-film transistors (OTFTs) are used as promising device platforms owing to their data handling capacity on integrated circuits, mechanical durability and flexibility, and printing processability[5]. More importantly, OTFTs can be integrated with transmitting systems, meaning that the big-data construction of bioactive data can be realized by using OTFTs as wearable biosensors. Furthermore, it is possible to compare and accumulate physiological information obtained from each person. Therefore, OTFT-based biosensors can also contribute to the expansion of basic medical research. In fact, the monitoring of biophysical or biochemical information by using flexible OTFTs has been widely reported[6,7]. OTFT characteristics are affected by charges of adsorbed molecules onto the surfaces of the semiconductor layer or terminal electrodes. Although the origins of the shifts in threshold voltage (ΔV_{TH}) in OTFT (FET)-based sensors have still been debatable, the researchers in the field of OTFT-based sensors have still used ΔV_{TH} as the sensing parameter. For example, it has been reported ΔV_{TH} stemmed from the adsorption of gas molecules onto the metal–ligand complex-based organic semiconductor[8]. Furthermore, there are many reports that the adsorbed biomolecules (e.g., nucleotides) onto the semiconductor or the gate electrode not only affect ΔV_{TH} but also induce changes in other parameters such as drain current (I_{DS}), the field-effect mobility (μ), etc.[9,10]. These demonstrated results indicate that the parameters of OTFT devices can be experimentally utilized for the sensing of signals for the determination of captured analytes. However, the detectable signals of previously reported devices were restricted to vital signs and changes in concentrations of small molecules, in spite of the fact that proteins are important biomarkers related to the onset of various diseases. To obtain accurate and reproducible sensing signals of targets, the alignment of analytes on devices should be tuned by molecular recognition materials. This is because ΔV_{TH} of OTFT-based sensors by adding target proteins are unstable in the physical adsorption model of proteins on the electrode surface. In the physical adsorption model, the adsorbed amount of proteins onto the electrode fluctuate owing to its non-specificity. In addition, the variability of ΔV_{TH} is also derived from various charge distributions of proteins (see Supplementary Fig. 1a). In contrast, the antibody-modified electrode can detect proteins based on the specific immune-interaction (see Supplementary Fig. 1b, c), which means that the adsorbed amount of target proteins on the electrode surface can be defined by the binding affinity and the immobilized amount of the antibody. Importantly, the distribution of surface charge on proteins is not homogeneous because acidic and basic amino-acids are placed on the protein surface heterogeneously. Hence, the well-ordered immobilization of the antibody on the electrode (i.e., alignment for the orientation of the captured protein) is required for achieving the accurate and reproducible detection of proteins (see Supplementary Fig. 1c). These suggest that the surface design of sensing electrodes is crucial to obtain the biomolecule information. Furthermore, self-assembled monolayer (SAM)-modified electrode can protect the non-specific adsorption of proteins and interferences on the electrode. Therefore, this standpoint from molecular recognition chemistry is important to achieve the accurate quantitative determination of biomarkers by using OTFTs. Toward this end, molecular recognition researchers have already established a strategy for achieving these requirements of protein detection[11–13]; nevertheless, suitable materials and functionalization for wearable sensors for the detection of proteins have not been considered in the field of device engineering. In this regard, although we have carefully examined the protein sensing ability of OTFT devices functionalized with several sensing materials[14], further consideration of flexible and printed OTFTs for protein determination is required. This is because the development of flexible devices for biosensing is still in its infancy.

Herein, we realize a flexible disposable biosensor that can electrically detect an immunological marker protein by combining different standpoints and knowledge of device engineering and molecular recognition chemistry. In this paper, we propose a conceptual design of an immunosensor device on an ultra-thin film with potential applicability to wearable biomedical systems. The fabricated OTFT with a dual-gate configuration[15] (Fig. 1) showed excellent operation stability under electrical or mechanical loading. More importantly, the designed immunosensing portion achieved the quantitative detection of proteins on a printed OTFT with mechanical flexibility. The obtained results suggest that the proposed device structure, process, and applied materials will contribute to the achievement of OTFT-based biosensors with these attractive characteristics. Furthermore, our OTFT-based immunosensor was fabricated by printing processes, meaning it could be used in low-cost biomedical systems.

Results

Fabrication of a dual-gate OTFT on an ultra thin-film substrate. The external appearance and schematic of the flexible OTFT are shown in Fig. 1. The fabrication procedure for the ultra-thin-film device including printing processes was in accordance with our previous report (see the "Methods" section)[16]. The fabricated device was easily peeled from the support substrate after finishing the preparation process. The thickness of the ultra-thin-film substrate was 1 μm, resulting in the OTFT device having a total thickness of <3 μm. In this study, we employed a dual-gate structure for the OTFT as the basic structure for flexible biosensors. This is because dual-gate OTFTs have a practical configuration for biosensors owing to their excellent robustness to mechanical stresses and their reproducible operation under ambient conditions. More importantly, dual-gate OTFTs can be easily integrated into logic circuitry[17]. This suggests that the processing and transmission of biometric information could be achieved by using an electronic system integrated into a single chip.

To accomplish the electrical detection of analytes in aqueous media using the OTFT, the sensing portion should be separated
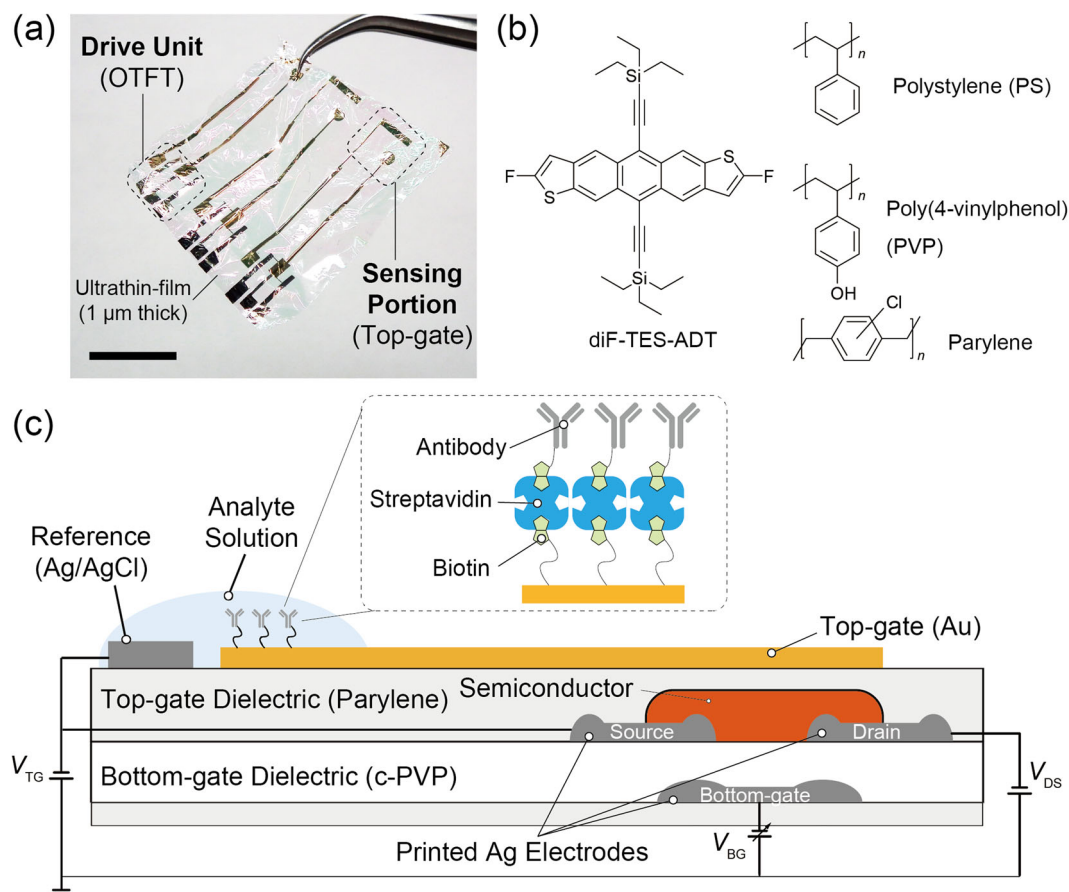
Fig. 1 Flexible OTFT-based immunosensor. a Photograph of the fabricated device. The scale bar is 1 cm. **b** Chemical structures of the utilized materials in this study. **c** Schematic illustration of an OTFT-based immunosensor on a 1-μm-thick film.

from the channel region of the OTFT because the electrical performance of organic semiconductors is easily deteriorated by exposure to water. Hence, the sensing electrode was extended apart from the area just above the semiconductor layer (Fig. 1)[18]. Consequently, we obtained excellent performance characteristics of the OTFT-based sensor as a consequence of this design strategy for the device (vide infra).

Electrical performance of the dual-gate OTFT. Basic operation behaviors (transfer and output characteristics) of the fabricated OTFT with the dual-gate configuration are summarized in Fig. 2 (see Supplementary Table 1). First, we carried out electrical measurements for the OTFT in the single-gate configuration (i.e., a top-gate or bottom-gate OTFT). Notably, the square roots of $|I_{DS}|$ versus V_{GS} in each device configuration exhibited as the linear behavior (see Supplementary Fig. 3), supporting that these analyzed results were highly reliable[19]. Next, the operation of the dual-gate OTFT was examined by applying the gate bias at both the top-gate and bottom-gate terminals (Fig. 2c). Figure 2d shows the correlation between the threshold voltage (V_{TH}) of the OTFT and the external sweep bias for the top-gate terminal (V_{TG}). A linear relationship between the output parameter (V_{TH}) and the input signal (V_{TG}) was observed, suggesting that the fabricated OTFT can be applied to the sensitive detection of the molecular recognition behavior on the top-gate electrode. Notably, the low-voltage operation of the fabricated OTFT with the single-gate or dual-gate configuration was observed (Fig. 2d). The application of high electric fields to water may affect various electrochemical reactions, such as the electrolysis and electrophoresis of charged molecules in the water. These uncontrollable

phenomena in the analyte solution might interfere with the read out of sensing signals from the solution. Thus, the device can be utilized for sensing applications because its low operation voltage can limit the occurrence of undesirable electrochemical reactions in aqueous media.

To evaluate the operation stability of the OTFT under long-term use, direct-current (DC) bias-stress measurement was also carried out for the fabricated device (Fig. 2e). Here, it is unnecessary for the bottom-gate portion of the designed OTFT to have stability under long-term continuous bias. This is because the intermittent operation of the bottom-gate device is sufficient for the read out of biosensing information from changes in the electrical potential of the top-gate terminal. Hence, we only evaluated the operation stability of the bottom-gate device under the application of continuous bias stress to the top-gate terminal. The transfer characteristics obtained under stress at a constant bias voltage ($V_{TG} = 0$ V) were employed to calculate and evaluate the changes in threshold voltage (ΔV_{TH}, Fig. 2f), field-effect mobility (μ/μ_0, Fig. 2f), and drain current (I_{DS}/I_{DS0}, Fig. 2g). Although a slight shift of the transfer characteristic was observed, the electrical parameters of the fabricated device were almost unaffected by the bias stress under ambient conditions.

Mechanical durability of the flexible OTFT. To determine the feasibility of future wearable sensors based on the OTFT, the mechanical durability of the flexible OTFT (Fig. 3a) was evaluated with bending and compression stress tests. Initially, bending stresses were applied to the OTFT as shown in Fig. 3b. The transfer characteristics of the dual-gate OTFT scarcely changed during the application of tensile stress (Fig. 3c). Hence, no
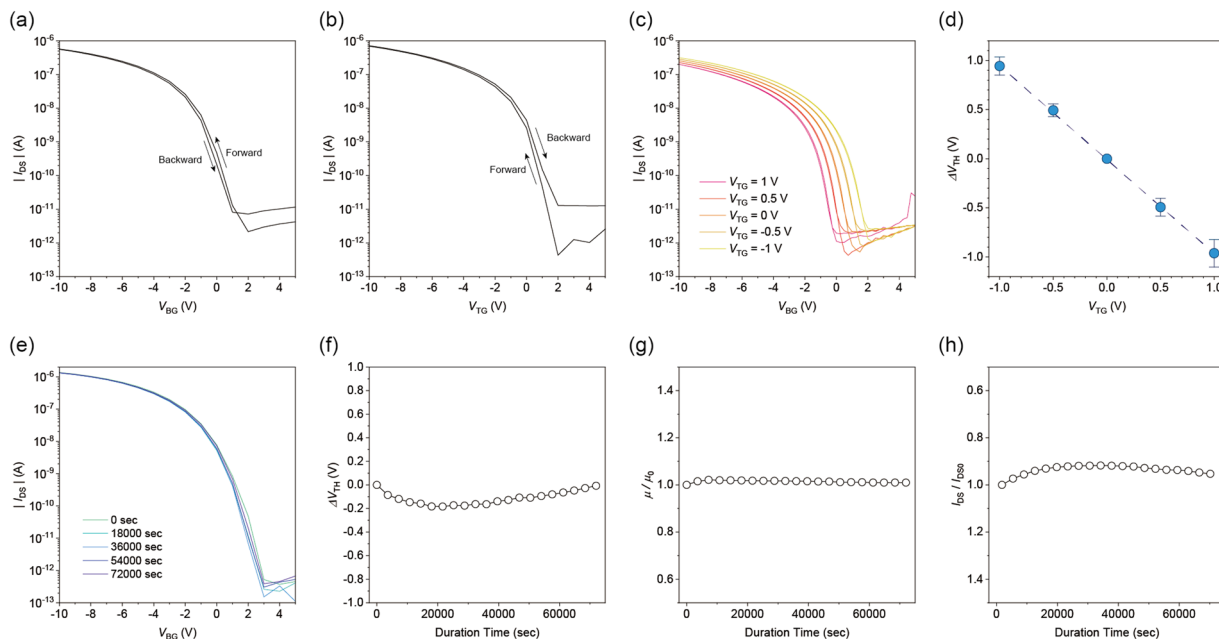
Fig. 2 Basic properties of the fabricated OTFT. $|I_{DS}|$–V_{GS} curves (transfer characteristics) of the fabricated OTFTs controlled by applying a single-gate voltage at **a** bottom-gate terminal (V_{BG} = +5 to −10 V) and **b** top-gate terminal (V_{TG} = +5 to −10 V) (V_{DS} = −1 V). **c** Transfer characteristics of the dual-gate OTFT (V_{DS} = −1 V). The applied V_{TG} was −1, −0.5, 0, 0.5, or 1 V. **d** Threshold voltage (V_{TH}) dependence with V_{TG} for the bottom-gate OTFT. **e** Transfer characteristics of the OTFT device taken before and after applying a constant bias voltage for 72,000 s (=20 h). **f**–**h** Changes in the electrical parameters [(**f**) threshold voltage, (**g**) field-effect mobility, and (**h**) drain current] of the fabricated OTFT device under DC bias stress.

changes in V_{TH} and mobility were obtained from the transfer curves of the ultra-thin-film device when bending stress was applied at each radius of curvature (Fig. 3d). Secondly, the electrical performance of the OTFT was measured under compressive strain (Fig. 3e). Although the device exhibited stable operation when applying stress with compression up to 15% (Fig. 3f, g), the device was broken under higher compressive stress (>20%). This phenomenon might be due to the materials employed in the flexible OTFT (vide infra). Fortunately, the durability observed upon applying each stress was sufficient for the electrical device to be mounted on human skin[20]. In other words, the device structure of the designed OTFT can be used as a wearable biosensing platform.

Confirmation of the biotin–streptavidin complexation on the top-gate electrode. Encouraged by the stable low-voltage operation of the OTFT, we decided to use the designed device for biosensing applications. Herein, we constructed a protein-sensing portion on the top-gate electrode by using the biotin–streptavidin complex as the sensing scaffold. Owing to the extremely high affinity of biotin (also known as vitamin B$_7$) to streptavidin ($K_d \sim 10^{-15}$ M), the system is often utilized to evaluate the sensing abilities of newly developed sensors. Furthermore, immobilized antibodies on substrate surfaces can be aligned by the biotin–streptavidin system[21], which indicates that the accuracy of immunosensors could be improved by using a biotin–streptavidin-complex-based scaffold.

To evaluate the sensing capability of the OTFT for a specific interaction, the sensing portion (the extended area of the top-gate electrode) of the OTFT was decorated by a biotin-terminated SAM (biotin–SAM). Then, a phosphate-buffered saline (PBS) solution with streptavidin was added dropwise to the top-gate electrode, and the transfer characteristic of the OTFT was subsequently measured. To confirm the decoration, we performed the surface characterization of the top-gate electrode (see Supplementary Fig. 9). Water contact angle goniometry (WCAG)

measurement revered a marked increase in the hydrophilicity of the biotin-modified top-gate electrode (Θ_W = 26°) upon its reaction with streptavidin (Θ_W = 10°) in comparison with that of an untreated gold film (Θ_W = 43°), indicating that the gold surface was covered with hydrophilic molecules (i.e., the biotin–SAM and/or the streptavidin protein) (see Supplementary Fig. 9). In addition, photoemission yield spectroscopy (PYS) measurement showed a slight shift in the depth direction for the work function from the untreated electrode (4.7 eV) to the SAM-modified electrode (4.8 eV), suggesting that the top-gate surface was treated with the electronegative group (i.e., the carboxy moiety of biotin) of the SAM (see Supplementary Fig. 9). The observed slope change in the PYS spectrum of the electrode after treatment with streptavidin implies that the emission of photoelectrons from the gold surface was suppressed by the adsorbed macromolecules (streptavidin) on the gold film. Furthermore, we carried out a direct observation of the functionalized electrodes by atomic force microscopy (AFM) measurement (see Supplementary Fig. 10). As expected, the surface topographies of the electrodes showed different expressions with each functionalization. Importantly, the obtained changes in topography agreed with those in a previous study[22]. From these characterization results, we concluded that the biotin–streptavidin complexation on the electrode was successful. Then, we carried out titration for streptavidin using the OTFT modified with the biotin–SAM. The fabricated OTFT responded predictably to the addition of streptavidin to the PBS solution at pH 7.0 (see Supplementary Fig. 11). The observed positive shift of the transfer characteristic with increasing streptavidin level showed that negatively charged molecules (i.e., streptavidin with the mildly acidic isoelectric point, pI ~ 5) were captured on the surface of the top-gate electrode.

Label-free electrical immunoassay for immunoglobulin G (IgG). Finally, to demonstrate the biosensing ability of the designed OTFT, we executed an immunoassay for IgG, which is

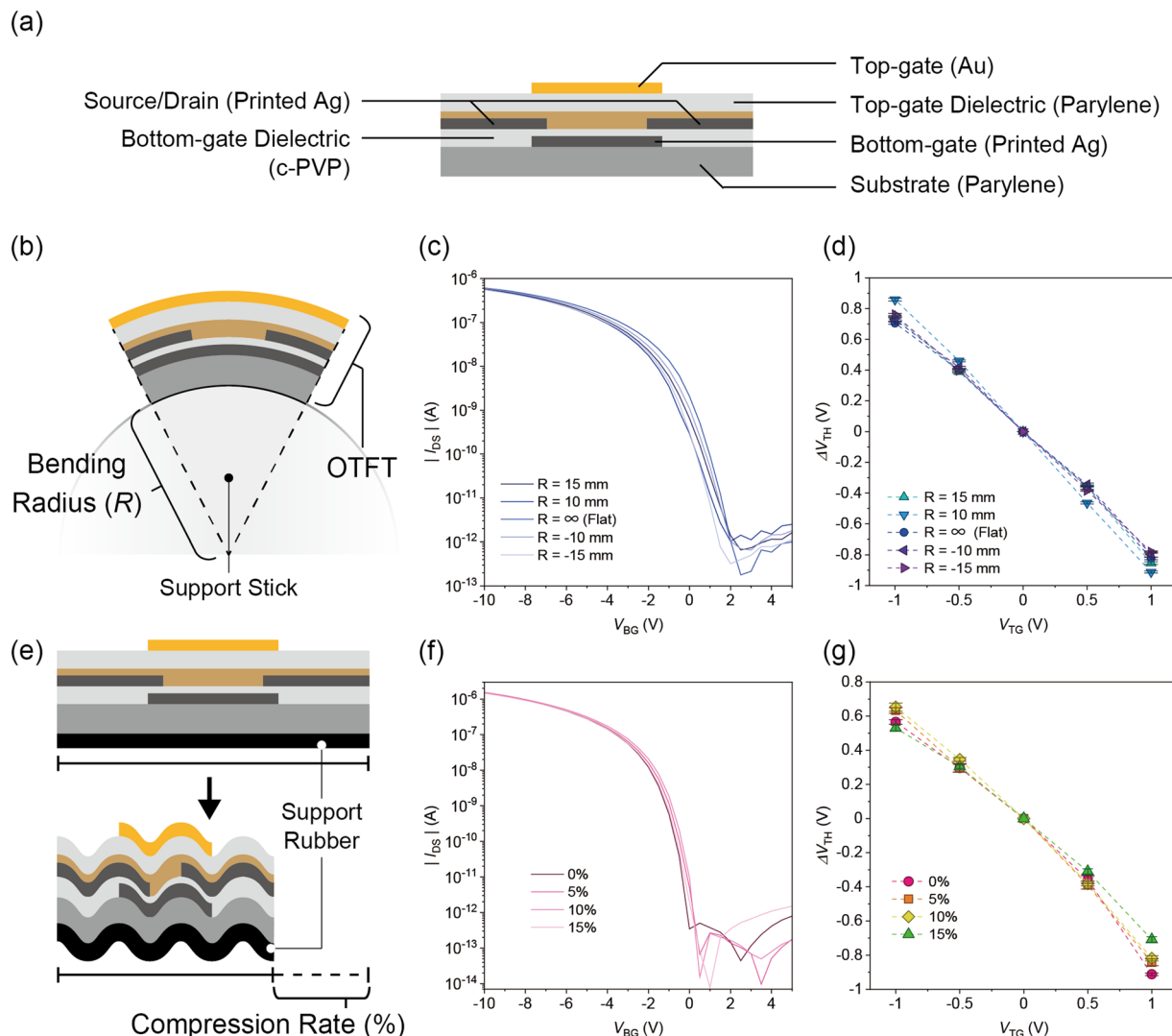**Fig. 3 Mechanical durability of the flexible OTFT. a** Diagram of the flexible OTFT. **b** Illustration of the flexible OTFT device under tensile strain. **c** Transfer characteristics of the fabricated OTFT before, during, and after application of bending stress. The applied V_{TG} was kept at 0 V. **d** Changes in the threshold voltage (V_{TH}) of the dual-gate OTFT at each radius of curvature. The number of measurement cycles for each condition was five. **e** Illustration of the flexible OTFT device upon applying compressive stress. **f** Transfer characteristics of the OTFT device before, during, and after application of compressive stress. The applied V_{TG} was kept at 0 V. **g** Changes in the threshold voltage (V_{TH}) of the dual-gate OTFT at various compression rates (0%, 5%, 10%, and 15%). The number of measurement cycles for each condition was five.

known as a biomarker protein for rheumatoid arthritis, infectious diseases, and inflammations[23]. Although immunoassays are some of the most general analytical methods for target proteins due to their high specificity, it is relatively complicated to use conventional immunoassays (e.g., enzyme-linked immunosorbent assays) to determine analyte information because of the necessity to label target proteins. Therefore, the development of label-free immunoassays utilizing flexible OTFTs is required to achieve the real-time monitoring of biomarker levels. In this study, a biotinylated polyclonal antibody was utilized as a label-free protein receptor for IgG on the top-gate sensing electrode treated with the biotin-terminated SAM/streptavidin complex (Fig. 4a). The protocol for the immunoassay is described in the "Methods" section. Figure 4b exhibits the titration results of the IgG protein, showing the observed shifts of V_{TH} with increasing IgG level. Note that the quantification of interfacial states between the top-gate electrode and the aqueous solution in FET-based sensors is difficult. For example, electrolyte conditions strongly affect the

interfacial potentials at the electrode surface. Although this point is well understood in the field of surface science, there may be cases where it differs from actual results[24]. This is because the reference plane on prepared electrodes is generally unclear owing to the complicated distributions in shape and charge of proteins. Hence, it is difficult to determine the valid value of the Debye length (i.e., the region influenced by electrolyte conditions) from the electrode unambiguously. Furthermore, the changes in electrical potential at the interface might also be triggered by the modulation of the dipole moment in the immobilized complex which consists of antibody, streptavidin, and the biotin–SAM on the electrode[25]. Nevertheless, the charge of the captured molecules on the device is one way of determining the driving force of electrical responses in FET-based sensors. Hence, the shifts of V_{TH} of the prepared device with increasing IgG level (Fig. 4b and Supplementary Fig. 12) are probably due to the shift of the electrical potential at the top-gate/solution interface. Hence, a positively charged IgG protein might be captured on the
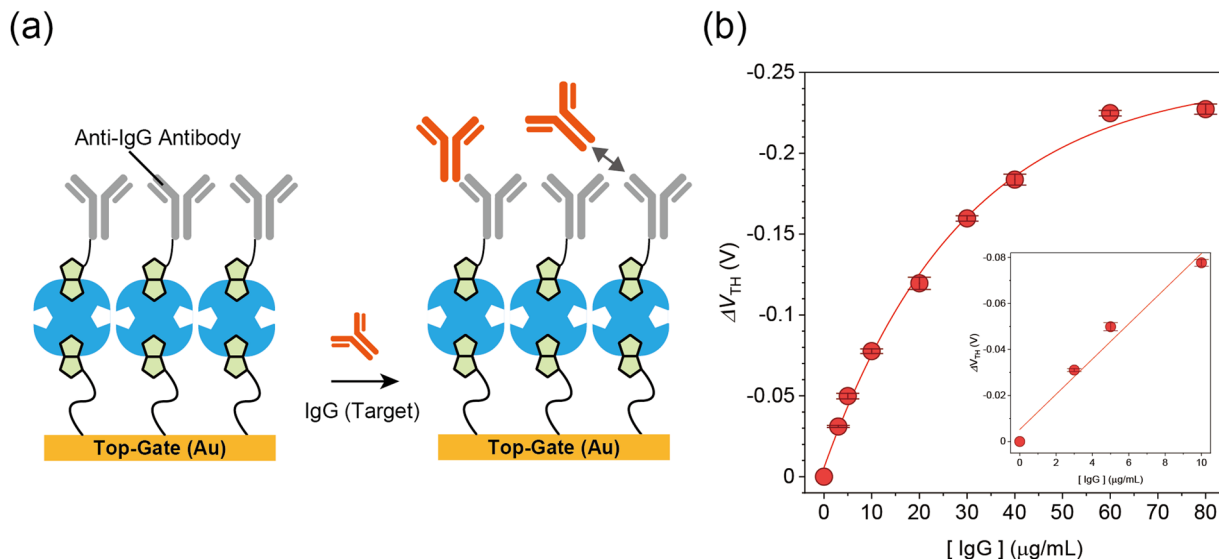
Fig. 4 Label-free immunoassay for IgG. a Schematic illustration of the sensing portion on the top-gate electrode modified with anti-IgG antibody. **b** Changes in the threshold voltage (V_{TH}) of the OTFT induced by the IgG protein at each concentration in a PBS solution with 0.1 wt% BSA. The number of measurement cycles for each condition was five.

top-gate sensing electrode (see Supplementary Fig. 1). More importantly, the titration experiment was successfully carried out in the presence of a large amount of bovine serum albumin (BSA, 0.1 wt%) as a protein interferent. Thus, the obtained electrical responses were derived from the specific molecular interaction between the target IgG and the antibody on the top-gate electrode.

Discussion

The fabricated OTFT was composed of printed materials and an ultra-thin-film substrate, and the device exhibited both operation stability and mechanical durability due to its adopted configuration (top-gate structure). First, the channel region of the OTFT was fully shielded by the top-gate dielectric (parylene film), resulting in the environmental robustness of the fabricated OTFT against the diffusion of water or oxygen into the semiconductor film[26]. In fact, even though all the measurements were performed under atmospheric conditions, the fabricated device showed excellent electrical performance characteristics. Second, the semiconductor layer was embedded at a neutral strain position in the fabricated device, i.e., sandwiched between both parylene layers (the top-gate dielectric and the substrate). Here, the calculated distance of the neutral strain position (r_n) from the bottom plane of the parylene film substrate was very close to the bottom-gate and top-gate channel regions (see Supplementary Fig. 7). In previous studies[27–30], it was demonstrated that an appropriate sandwich structure can contribute to the suppression of a compressive or tensile strain at the neutral strain position. Therefore, we concluded that the excellent mechanical durability during the device operation is owing to the appropriate structure for suppressing mechanical strains on both channel planes (i.e., the interfaces between the semiconductor and each dielectric layer). Consequently, we concluded that the designed OTFT has excellent mechanical stability[27–30]. Because the maximum compression rate of human skin is around 20%[20,31], our results demonstrate that the fabricated device has sufficient robustness against compressive stress, although the device broke above a compressive strain of 20%. Incidentally, the origin of the malfunction of the OTFT subjected to more than 20% compressive strain might have been due to the contact between the polycrystalline organic

semiconductor and the dielectric films[32]. These results show that the designed OTFT with the top-gate configuration has satisfactory characteristics for the development of wearable biosensors to monitor biomarker behaviors in real time.

In conclusion, we have successfully demonstrated the biosensing abilities of a printed dual-gate OTFT on a 1-μm-thick film. Our fabricated device electrically responded to increasing biomolecule concentrations on the sensing electrode. The sensitivity of the ultra-thin-film immunosensor device to IgG (linear response range: 0–10 μg/mL) was comparable to that of conventional immunoassays including TFT-based immunosensors (see Supplementary Table 2). Notably, biosensing was accomplished even in the presence of a protein interferent, suggesting that the designed immunosensor can rapidly detect biomarkers in body fluids without any pretreatments. In addition, while the ionic compositions of the PBS solution and a biological fluid (e.g., sweat) are slightly different, the ionic strength of the PBS solution is much higher than the concentration of the ionic interferent in sweat (see Supplementary Table 3). Hence, the obtained result indicates that the fabricated device can sensitively monitor changes in marker levels in sweat on the human skin. Moreover, OTFT-based sensors can detect electrical charges of captured proteins statically and directly. This suggests that OTFTs are more suitable platforms for constructing protein-sensing systems than conventional electrochemical sensors[8,10]. General electrochemical sensors detect electron transfer associated with oxidation or reduction of target molecules. Therefore, these types of sensors can sensitively detect targets in the ideal electrolyte system. However, the electrochemical detection of protein markers is difficult due to the following reasons: (1) since proteins are composed of various amino acids with different electrical potentials, electrochemical peaks derived from these amino-acid residues interfere with each other. In addition, biological fluids including proteins contain various types of electrolytes at high concentrations. From these matters, it is difficult to secure the selectivity and sensitivity in electrochemical sensors for protein analyses. (2) Electrochemical stimulation breaks higher-ordered structures and minute residue sequences in proteins. This means that the accurate analysis of protein markers by electrochemical methods is difficult. Whereas, FETs (including OTFTs) can detect

charge of captured proteins without irreversible electrochemical reactions. (3) Amperometric sensors are incapable of the detection of redox-inactive proteins. In addition, although sensing electrodes should cover redox potentials of target proteins, the electrochemical window of typical electrode materials is narrower than high-potential peaks derived from proteins. Therefore, we concluded that OTFT-based sensors are some of the suitable platforms for the detection of proteins compared to electrochemical measurements. On the basis of these points, we believe that our proposed strategy to develop the OTFT-based immunosensor with printed components could pave the way to a new approach for disposable and wearable biosensors for the on-site detection of various biomarkers.

Methods

General. All solvents and reagents employed for this research were used as supplied. More details are given in Supplementary Methods.

Device fabrication. The device structure of the dual-gate OTFT is shown in Fig. 1. First, an amorphous fluoropolymer (DuPont, Teflon AF1600) in a solution of a fluorinert solvent (3 M, FC-43) was coated on a glass substrate at a rotation speed of 2000 rpm for 60 s. The thickness of the fluoropolymer film was 210 nm. The substrate was baked on a hotplate at 150 °C for 1 h under ambient conditions. In this study, the fluoropolymer-deposited glass substrate was utilized as a supporting carrier for the preparation of the ultra-thin film device[13]. Then, a 1 μm-thick parylene thin film was deposited on the substrate using chemical vapor deposition (CVD) equipment. Afterward, a cross-linked poly(4-vinylphenol) (c-PVP) solution was spin-coated at a rotation speed of 4000 rpm for 1 min, and then the substrate was baked at 150 °C for 1 h in a N_2-filled glove box ([H_2O]: < 1 ppm, [O_2]: < 1 ppm). The c-PVP solution consisted of PVP (M_w: about 25,000) and a cross-linking agent [poly(melamine-co-formaldehyde), M_n: about 432] in propylene glycol monomethyl ether acetate. The c-PVP film was not only employed as a planarization layer for the surface of the parylene film, but also contributed to controlling the surface energy (droplet wettability) of the underlayer, enabling uniform and stable formation of laminated materials (i.e., a silver (Ag)-nanoparticle ink) on the substrate. Next, the c-PVP-film surface was treated with an O_2 plasma cleaner (Samco, PC-300). The treatment duration was 2 min and the plasma power was 100 W. Subsequently, a water-based Ag-nanoparticle ink (DIC, JAGLT-01) was used as the bottom-gate electrode and deposited on the substrate by using inkjet printer equipment (Fujifilm Dimatix, DMP-2831) with a 10 pL nozzle head. The dot-to-dot spacing for the droplet deposition was fixed at 60 μm, and the substrate temperature was kept at 30 °C during printing to form the bottom-gate layer. To planarize the electrode surface, the substrate was then stored in an environmental control chamber (ESPEC, SH-221) at 95% RH (=relative humidity) and 30 °C for 30 min[33]. To sinter the Ag nanoparticles, the printed bottom-gate layer was annealed at 120 °C for 1 h under ambient conditions. Next, a second c-PVP film was deposited on the printed gate electrode by the spin-coating (rotation speed: 2000 rpm). The second c-PVP film was utilized as the bottom-gate dielectric layer (film thickness: 450 nm). A tetradecane-based Ag-nanoparticle ink (Harima Chemicals, NPS-JL) was applied as the drain and source electrodes and patterned on the c-PVP dielectric film by the inkjet printer. These electrodes were printed under the same conditions as the bottom-gate electrode. The printed electrodes were sintered at 120 °C for 30 min in ambient air. To improve the carrier injection efficiency from the source to the semiconductor, the surface of the printed electrodes was dipped in a 2-propanol solution of perfluorobenzenethiol (PFBT, 30 mM) for 5 min, and then the substrate was rinsed with 2-propanol and dried with N_2 gas[34]. After this, a blend ink consisting of 2,8-difluoro-5,11-bis(triethylsilylethynyl)anthradithiophene (diF-TES-ADT, 2 wt%) and polystyrene (PS, M_w: ~280,000, 0.5 wt%) in mesitylene was used as an organic semiconductor layer and deposited in the aperture region between the drain and source electrodes (channel area) by using dispensing equipment (Musashi Engineering, IMAGEMASTER 350). The diF-TES-ADT material was synthesized in accordance with the literature[35]. A parylene-based top-gate dielectric was then formed on the substrate (thickness: 500 nm). We utilized the parylene film as the top-gate dielectric because the CVD process can completely cover the rough surface of the underlayer, i.e., the crystalline semiconductor (diF-TES-ADT). Next, a gold (Au) film was formed on the parylene dielectric layer by resistance heating evaporation at a rate of 0.1–0.5 Å s^{-1} under a pressure of 10^{-4} Pa (thickness: 50 nm). The Au thin film was utilized as extended top-gate and control-gate (pseudo-reference) electrodes. The control gate was covered with Ag/AgCl paste. Finally, the completed device was peeled from the glass substrate. Importantly, the parylene film can be easily peeled from the supporting carrier owing to the high release performance of the amorphous fluoropolymer film (surface energy: about 8.1 mN m^{-1}).

Modification of the immune-sensing electrode. First, an ethanol solution containing 1 mM biotin–SAM formation reagent (Dojindo, B564) was added dropwise on the Au top-gate electrode at room temperature (reaction time: 1 h). After washing the

top-gate electrode with ethanol and water, a PBS (Sigma-Aldrich, D8537) solution of 500 μg/mL streptavidin was casted on the biotin-modified electrode for 15 min at room temperature. Afterward, a PBS solution of the biotinylated antibody for IgG (30 μg/mL) with 0.1 wt% bovine serum albumin (BSA) protein and 0.05 wt% Tween 20 surfactant was cast and incubated on the top-gate electrode modified with streptavidin at room temperature (incubation time: 30 min). Then, the sensing electrode was washed with the PBS solution. The characterization results for the extended top-gate electrode are summarized in Supporting Information.

Label-free immunoassay. The PBS solution of the IgG (0–80 μg/mL) with the BSA additive (0.1 wt%) was added dropwise on the extended top-gate electrode and incubated at 37 °C (incubation time: 1 h). Then, the IgG was electrically detected by the dual-gate OTFT without further treatment.

Characterization of the fabricated device. The electrical properties of the fabricated device were analyzed using a semiconductor parameter analyzer (Keithley, 4200-SCS). All measurements were performed under atmospheric conditions. The basic characteristics of the fabricated OTFT were measured before the peeling of the device from the supporting substrate. To investigate the mechanical durability of the fabricated OTFT, the tensile strain or compressive stress was applied to the device by using a support stick or rubber (Fig. 3b, e). Here, the flexible OTFT was carefully peeled from the support substrate (the glass plate). However, ΔV_{TH} of the OTFT was slightly different before (Fig. 2d) and after (Fig. 3d) the peeling process of the device from the supporting substrate. Although the OTFT device might be slightly damaged by the process, the peeled OTFT operated reproducibly in this study. The work function of the Au-sensing electrodes was analyzed by photoemission yield spectroscopy in air (PYS, Riken Keiki, AC-3). The surface wettability of the Au films was determined using a contact angle goniometer (CAG, Biolin Scientific, Theta T200). The surface topography of the sensing electrode at each modification step was collected by AFM (Shimadzu Corp., SPM-9700).

Data availability

The datasets that support all the findings of this study are available from the corresponding authors upon reasonable request.

References

1. Tu, J., Torrente-Rodríguez, R. M., Wang, M. & Gao, W. The era of digital health: a review of portable and wearable affinity biosensors. *Adv. Funct. Mater.* **30**, 1906713 (2020).
2. Seshadri, D. R. et al. Wearable sensors for monitoring the physiological and biochemical profile of the athlete. *NPJ Digit. Med.* **2**, 72 (2019).
3. Bandodkar, A. J. et al. Battery-free, skin-interfaced microfluidic/electronic systems for simultaneous electrochemical, colorimetric, and volumetric analysis of sweat. *Sci. Adv.* **5**, eaav3294 (2019).
4. Gao, W. et al. Fully integrated wearable sensor arrays for multiplexed in situ perspiration analysis. *Nature* **529**, 509–514 (2016).
5. Li, H. et al. Chemical and biomolecule sensing with organic field-effect transistors. *Chem. Rev.* **119**, 3–35 (2019).
6. Ray, T. R. et al. Bio-Integrated wearable systems: a comprehensive review. *Chem. Rev.* **119**, 5461–5533 (2019).
7. Wang, N., Yang, A., Fu, Y., Li, Y. & Yan, F. Functionalized organic thin film transistors for biosensing. *Acc. Chem. Res.* **52**, 277–287 (2019).
8. Andringa, A.-M. et al. Gas sensing with self-assembled monolayer field-effect transistors. *Org. Electron.* **11**, 895–898 (2010).
9. Boileau, N. T., Melville, O. A., Mirka, B., Cranston, R. & Lessard, B. H. P and N type copper phthalocyanines as effective semiconductors in organic thin-film transistor based DNA biosensors at elevated temperatures. *RSC Adv.* **9**, 2133–2142 (2019).
10. Minami, T., Minamiki, T. & Tokito, S. Electric detection of phosphate anions in water by an extended-gate type organic field-effect transistor functionalized by a zinc(II)–dipicolylamine derivative. *Chem. Lett.* **45**, 371–373 (2016).
11. Lin, J. & Ju, H. Electrochemical and chemiluminescent immunosensors for tumor markers. *Biosens. Bioelectron.* **20**, 1461–1470 (2005).
12. Haas, K. L. & Franz, K. J. Application of metal coordination chemistry to explore and manipulate cell biology. *Chem. Rev.* **109**, 4921–4960 (2009).
13. Minamiki, T., Kubota, R., Sasaki, Y., Asano, K. & Minami, T. Protein assays on organic electronics: rational device and material designs for organic transistor-based sensors. *ChemistryOpen* **9**, 573–581 (2020).
14. Kubota, R., Sasaki, Y., Minamiki, T. & Minami, T. Chemical sensing platforms based on organic thin-film transistors functionalized with artificial receptors. *ACS Sens.* **4**, 2571–2587 (2019).

15. Spijkman, M.-J. et al. Dual-gate thin-film transistors, integrated circuits and sensors. *Adv. Mater.* **23**, 3231–3242 (2011).
16. Fukuda, K. et al. Fully-printed high-performance organic thin-film transistors and circuitry on one-micron-thick polymer films. *Nat. Commun.* **5**, 4147 (2014).
17. Jang, H.-J. & Cho, W.-J. Performance enhancement of capacitive-coupling dual-gate ion-sensitive field-effect transistor in ultra-thin-body. *Sci. Rep.* **4**, 5284 (2014).
18. Minamiki, T. et al. Accurate and reproducible detection of proteins in water using an extended-gate type organic transistor biosensor. *Appl. Phys. Lett.* **104**, 243703 (2014).
19. Choi, H. H., Cho, K., Frisbie, C. D., Sirringhaus, H. & Podzorov, V. Critical assessment of charge mobility extraction in FETs. *Nat. Mater.* **17**, 2–7 (2018).
20. Zhou, B., Xu, F., Chen, C. Q. & Lu, T. J. Strain rate sensitivity of skin tissue under thermomechanical loading. *Philos. Trans. R. Soc. A* **368**, 679–690 (2010).
21. Lai, C.-H. et al. Site-specific antibody modification and immobilization on a microfluidic chip to promote the capture of circulating tumor cells and microemboli. *Chem. Commun.* **53**, 4152–4155 (2017).
22. Taninaka, A., Takeuchi, O. & Shigekawa, H. Reconsideration of dynamic force spectroscopy analysis of streptavidin–biotin interactions. *Int. J. Mol. Sci.* **11**, 2134–2151 (2010).
23. Kay, R. A., Wood, K. J., Bernstein, R. M., Holt, P. J. L. & Pumphrey, R. S. H. An IgG subclass imbalance in connective tissue disease. *Ann. Rheum. Dis.* **47**, 536–541 (1988).
24. Chu, C.-H. et al. Beyond the Debye length in high ionic strength solution: direct protein detection with field-effect transistors (FETs) in human serum. *Sci. Rep.* **7**, 5256 (2017).
25. Credo, G. M. et al. Label-free electrical detection of pyrophosphate generated from DNA polymerase reactions on field-effect devices. *Analyst* **137**, 1351–1362 (2012).
26. Nam, S. et al. Solvent-free solution processed passivation layer for improved long-term stability of organic field-effect transistors. *J. Mater. Chem.* **21**, 775–780 (2011).
27. Sekitani, T. et al. Ultraflexible organic field-effect transistors embedded at a neutral strain position. *Appl. Phys. Lett.* **87**, 173502 (2005).
28. Sekitani, T., Zschieschang, Z., Klauk, H. & Someya, T. Flexible organic transistors and circuits with extreme bending stability. *Nat. Mater.* **9**, 1015–1022 (2010).
29. Kim, D.-H. et al. Stretchable and foldable silicon integrated circuits. *Science* **320**, 507–511 (2008).
30. Fukuda, K. et al. Strain sensitivity and durability in p-type and n-type organic thin-film transistors with printed silver electrodes. *Sci. Rep.* **3**, 2048 (2013).
31. Annaidh, A. N., Bruyère, K., Destrade, M., Gilchrist, M. D. & Otténio, M. Characterization of the anisotropic mechanical properties ofexcised human skin. *J. Mech. Behav. Biomed.* **5**, 139–148 (2012).
32. Wang, X. et al. A universal strategy to improve the mechanical stability of flexible organic thin film transistors. *J. Mater. Chem. C* **7**, 6323–6331 (2019).
33. Fukuda, K., Sekine, T., Kumaki, D. & Tokito, S. Profile control of inkjet printed silver electrodes and their application to organic transistors. *ACS Appl. Mater. Interfaces* **5**, 3916–3920 (2013).
34. Takeda, Y. et al. Fabrication of ultra-thin printed organic TFT CMOS logic circuits optimized for low-voltage wearable sensor applications. *Sci. Rep.* **6**, 25714 (2016).
35. Subramanian, S. et al. Chromophore fluorination enhances crystallization and stability of soluble anthradithiophene semiconductors. *J. Am. Chem. Soc.* **130**, 2706–2707 (2008).

Author contributions
T. Minamiki, T. Minami, K.F. and S.T. designed the research and experiments. T. Minamiki, Y.-P.C., Y.T., and T.M. carried out the experimental work and data analysis. T. Minamiki, T. Minami, and S.T. wrote the manuscript incorporating comments from all authors.

Competing interests
The authors declare no competing interests.

Additional information
Supplementary information is available for this paper at https://doi.org/10.1038/s43246-020-00112-z.

Correspondence and requests for materials should be addressed to T.M. or S.T.

Peer review information Primary handling editors: Jie Xu, John Plummer.

Reprints and permission information is available at http://www.nature.com/reprints

Publisher's note Springer Nature remains neutral with regard to jurisdictional claims in published maps and institutional affiliations.